Downloaded 09/04/22 to 204.124.181.130. Redistribution subject to SEG license or copyright; see Terms of Use at http://library.seg.org/page/policies/terms
DOI:10.1190/image2022-3737841.1

# 3D real-time imaging for electromagnetic fracturing monitoring based on deep learning

*Zhigang Wang, Yao Lu*, BGP, CNPC;*
*Ying Hu, Yinchu Li, Ke Wang, Dikun Yang, The Department of Earth and Space Sciences, Southern University of Science and Technology*

## Summary

The electromagnetic method has a proven physical basis and advantages in subsurface fluid detection. The result of fracturing operation can be evaluated by monitoring the electromagnetic anomalies from low-resistivity fracturing fluid before and after the fracturing and inferring the range of fracturing fluid distribution. However, the traditional electromagnetic 3D inversion is time-consuming and cannot meet the requirement of real-time imaging during fracturing. In this paper, we use an improved supervised deep fully convolutional network (FCN) to learn the relationship between surface electromagnetic data patterns and the underground fracturing fluid distribution models. The relationship is encoded in many synthetic "data-model" pairs obtained through 3D forward modeling. By completing the forward modeling and neural network training on the computer cluster in advance, we successfully carried out a field experiment of 3D real-time imaging of fracturing fluid.

## Introduction

In the shale gas hydraulic fracturing production, fracture and fluid monitoring are important technical aspects that ensure production efficiency, extraction effectiveness and safety, and is essential for obtaining real-time information such as hydraulic fracturing stimulated zones and fracturing fluid distribution. The micro-seismic technique can accurately track fractures' location and magnitude in real time and has been widely used commercially. However, it is not always reliable to infer fracturing fluid migration state and evaluate the stimulated reservoir volume (SRV) of unconventional oil and gas reservoirs only based on the rock fracture information. In recent years, the traditional electromagnetic methods based on the high sensitivity to porosity and water saturation has shown advantages in subsurface fluid monitoring such as enhanced oil recovery, geothermal injection, and evaluation of hydraulic fracturing effects. However, the EM method is often plagued by several factors during multi-stage hydraulic fracturing of horizontal wells, such as weak electrical anomalies caused by the migration of small-volume fracturing fluid, high EM noise in the field, and lagging quantitative results due to time-consuming inversion calculations.

In recent years, Liu et al. (2019) studied the application of deep learning in resistivity inversion. Puzyrev et al. (2019) developed an FCN-based electromagnetic inversion algorithm to image the resistivity distribution of $CO_2$ storage area. Li et al. (2019), Colombo et al. (2020), Li et al. (2021) applied the U-net framework for 3D EM monitoring of fluids. The above research results demonstrate the real-time EM imaging method for fracturing monitoring based on deep learning is feasible. In addition, Li et al. (2021) used the equivalent resistor network approach (RESnet) to simulate the long steel cased well as an equipotential body for fast calculation of the EM response during fracturing monitoring. Hu et al. (2022) successfully simulated the EM response of a multi-well and multi-stage fracturing operation by the finite volume method (FVM). In this paper, we use this method to quickly generate training samples for deep learning in electromagnetic fracturing monitoring.

In this study, we introduce an improved supervised deep fully convolutional network (FCN) based imaging method that can take advantage of the long steel casings and ground-based time-frequency electromagnetic observation equipment (Wang et al., 2017, 2019) for real-time prediction of fracturing fluid distribution from ground observation data. The application was carried out at the shale gas fracturing site from stage 2 to 11 in a well in Sichuan, China. 3D real-time electromagnetic imaging was obtained for each fracturing stage. The results show the practical value of this method in quantitative monitoring of the injection, migration, flowback, and retention of fracturing fluid over time.

## Method

In this paper, a specific supervised fully convolutional network is designed based on conventional FCN and U-net for the imaging of different fluid distribution models (Figure 1). The blue arrow in Figure 1 represents a basic operation unit, successively a convolutional layer, a batch-normalization (BN) layer, and a nonlinear rectified linear unit (ReLU) activation function or layer. The red and green arrows indicate max-pooling and upsampling operations, respectively. The black arrows indicate the skip connection operations. Our network has seven sampling changes using three max-pooling and four upsampling layers, forming an asymmetric network structure. The surface electrical field data can be used as the input and the 3D fluid distribution


© 2022 Society of Exploration Geophysicists and the American Association of Petroleum Geologists

Downloaded 09/04/22 to 204.124.181.130. Redistribution subject to SEG license or copyright; see Terms of Use at http://library.seg.org/page/policies/terms
DOI:10.1190/image2022-3737841.1

model as the output (or label). This structure makes it possible for the fully convolutional networks to obtain the high-resolution image from the low-resolution data. Based on the above network architecture, we apply root mean square error (RMSE), adaptive moment estimation, and dropout as the loss function, optimizer, and regularization technique in deep learning, respectively (Li et al., 2021).

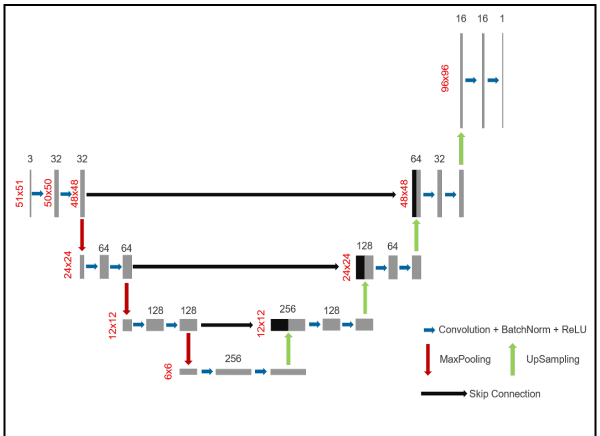


Figure 1: The specific architecture of the FCN in our imaging (Li et al., 2021)

During fracturing, the small-scale fracturing fluid is buried deeply. Fortunately, the mutual coupling between the target and survey configurations is helpful to amplify the electromagnetic anomaly caused by the directional flow of the fluid perpendicularly penetrated by the horizontal section of the well (Li et al., 2021; Hu et al., 2022). The fluid distribution is represented by an ellipsoid defined by nine randomly generated parameters (one equatorial radius, two polar radii, three azimuthal angles, and the central coordinates). Using the concept of edge conductivity (Hu et al., 2022), we can straightforwardly numerical model steel casing on a finely discretized mesh. With the aid of numerical simulations, we create a data set made of many fracturing fluid models and time-lapse data images. The training is performed on a workstation until the best network is formed. Then we can predict the imaging results of 3D fracturing fluid distribution by feeding the surface time-lapse data into the neural network.

## Example

The field experiment is located in a shale gas field in Sichuan, China. Eight wells exist at the site in parallel, forming a multi-well cluster. The application of the method was carried out in horizontal well #9 with the parallel horizontal sections at a depth of 2750m during the fracturing stage 1 to stage 11. The length of the horizontal section is about 2000 m. There are 13 survey lines directly above the fracturing area, and the length of each line is about 1200m. The electrical field in the x directions is measured every 50 m, and the electrode spacing is about 50 m. A total of 481 receivers were setup (Figure 2). Four kilometers of a grounded galvanic source (AB) are parallel to the survey line. The minimum and maximum offset are 3.5 and 4.6 km, respectively. A 100% duty cycle square wave with a 65-A current was transmitted at 20 different frequencies (Table 1).

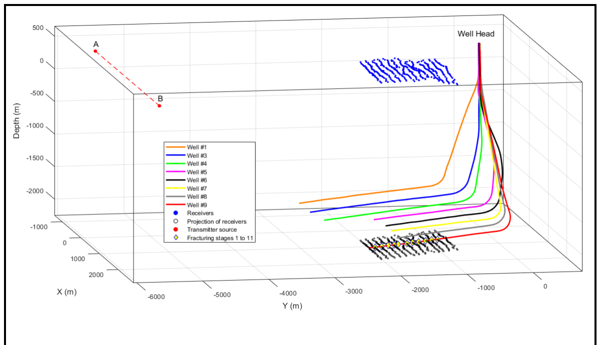


Figure 2: Positions of transmitter, receivers and horizontal wells in Sichuan, China

Table 1: Frequency table

| No. | Period (s) | Frequency (Hz) |
|---|---|---|
| 1 | 0.104 | 9.615385 |
| 2 | 0.142 | 7.042254 |
| 3 | 0.188 | 5.319149 |
| 4 | 0.25 | 4 |
| 5 | 0.35 | 2.857143 |
| 6 | 0.47 | 2.12766 |
| 7 | 0.63 | 1.587302 |
| 8 | 0.85 | 1.176471 |
| 9 | 1.13 | 0.884956 |
| 10 | 1.25 | 0.8 |
| 11 | 1.53 | 0.653595 |
| 12 | 2.05 | 0.487805 |
| 13 | 2.75 | 0.363636 |
| 14 | 3.71 | 0.269542 |
| 15 | 4.99 | 0.200401 |
| 16 | 6.73 | 0.148588 |
| 17 | 9.05 | 0.110497 |
| 18 | 12.15 | 0.082305 |

Downloaded 09/04/22 to 204.124.181.130. Redistribution subject to SEG license or copyright; see Terms of Use at http://library.seg.org/page/policies/terms
DOI:10.1190/image2022-3737841.1



First, the conductivities of the background formations are derived from well logging data, then we assign an equivalent edge conductivity to the string of vertical edges representing the steel casings (Hu et al., 2022). The location and directional flow range of fracturing fluid are estimated from the perforation data of each stage. We create a synthetic data set made of 3000 samples, including ellipsoidal models as output and the average relative difference of data between two consecutive stages as input. Those 3000 labeled samples are split into three parts before the training phase: the training data set (80%), the validation data set (10%), and the test data set (10%). In the training process, the parameters were adjusted according to the type of hidden-layer activation function, the presence or absence of the pooling layer, the size of the convolutional kernel, and the dropout rate. When the loss value no longer decays and reaches the minimum, the network is deemed trained. The above steps are completed on a workstation in advance, and the unique network will be saved for each fracturing stage.

Taking the fracturing stage 8 of well #9 under the frequency 0.65 Hz (1.53 s) as an example, we estimated that the coordinates of the fracturing fluid center were (1165.42m, -1251.29m, -2150m), the random-walk ranges of the three radii were 20m ~ 50m, 100m ~ 250m, and 20m ~ 50m, respectively, and the ranges of the three angles were 0 ~ 30 degree. Three thousand fracturing fluid distributions were randomly generated, and the inputs were obtained after 442 minutes of parallel forward calculation on the computer clusters.

We only selected the fracturing fluid region of stage 8 as the 3D imaging volume by cropping the conductivity model of the whole space. As a result, the dimension of the output (3D mesh) became 14 × 46 × 27. After preprocessing the observation data, we obtain gridded data image with 8 rows and 26 columns. The image size is consistent with the neural network's structure (Figure 3). We input the image into the neural network trained for the parameters of stage 8, and the location and distribution of the low resistance anomaly were predicted in 844 ms (Figure 4).

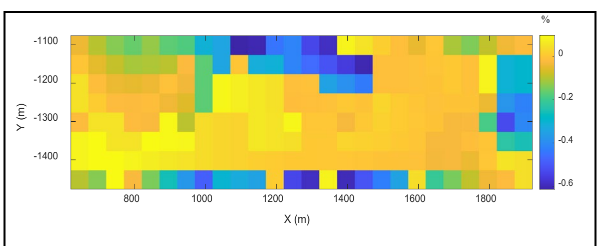


Figure 4: Image of real input data for neural network prediction in fracturing stage 8

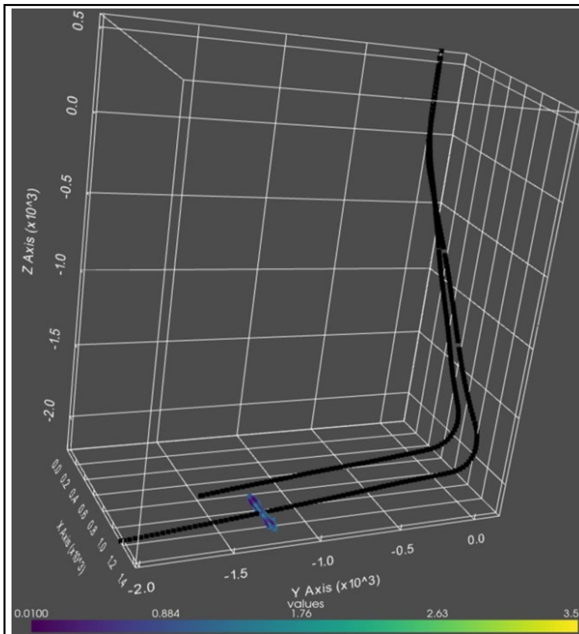


Figure 3: 3D real-time imaging result of EM fracturing monitoring in fracturing stage 8

The predictions of each stage can be used as the conductivities of the background formations when the next fracturing begins, and the inversions of all fracturing stages adopt the same workflow by training the network and predict over and over again. The imaging results of all fracturing stages at well #9 are shown together in Figure 5.


© 2022 Society of Exploration Geophysicists and the American Association of Petroleum Geologists

Downloaded 09/04/22 to 204.124.181.130. Redistribution subject to SEG license or copyright; see Terms of Use at http://library.seg.org/page/policies/terms
DOI:10.1190/image2022-3737841.1



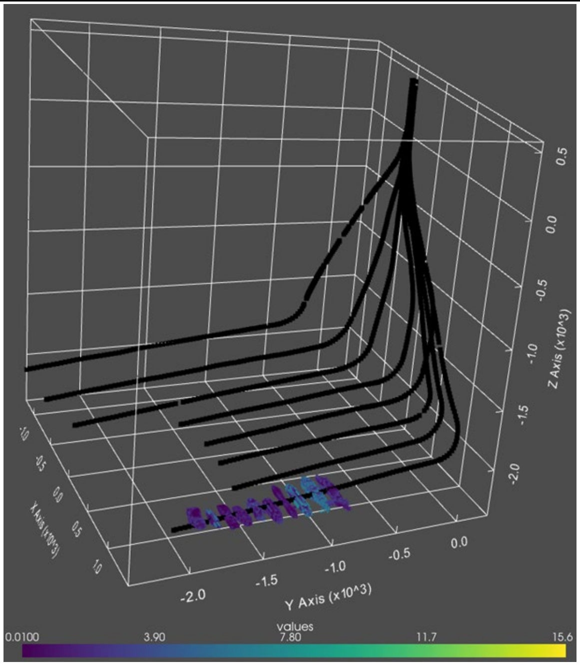


Figure 5: 3D real-time imaging result of EM fracturing monitoring at fracturing stage 2 to 11

The imaging results show a small distribution range of fracturing fluid at the early stages but more expanded in the late stages. The most probable cause is that the fracturing alternates between well #8 and the nearby well #9. Since the volumes of fracturing fluid and the underground connectivity are different at each stage, the predicted resistivity of each fracturing fluid unit is also different. This field survey shows the practicability and effectiveness of real-time imaging of electromagnetic fracturing monitoring based on deep learning. The performance of our technology meets the requirements for rapid imaging of the fracturing fluid.

## Conclusions

The research of this project has gained some new understanding of electromagnetic fracturing monitoring technology.

- The steel casings are the non-negligible good conductor and therefore need to be considered in EM simulation and fracturing monitoring.
- The deep learning method is helpful to obtain the monitoring results of fracturing in real time.
- The method based on a novel concept of edge conductivity can implement the 3D fast simulation with steel casing effects.

In the process of shale gas hydraulic fracturing, the 3D real-time imaging for EM fracturing monitoring using a deep-learning method utilizes the neural network trained in advance to rapidly predict the 3D distribution and geometry of fracturing fluid with the surface electromagnetic data acquired at each fracturing stage. The application of field data shows that the method can monitor the fracturing in real time, as well as providing practical values for capturing the dynamic distribution of fracturing fluid, predicting its directional flow, guiding subsequent fracturing schemes, and preventing accidents like casing deformation.

## Acknowledgments

This study was funded by BGP, CNPC Scientific Research Program.


© 2022 Society of Exploration Geophysicists and the American Association of Petroleum Geologists

## REFERENCES


Colombo, D., W. Li, E. Sandoval-Curiel, and G. W. McNeice, 2020, Deep-learning electromagnetic monitoring coupled to fluid flow simulators: Geophysics, **85**, no. 4, WA1–WA12, doi: https://doi.org/10.1190/geo2019-0428.1.

Hu, Y., D. Yang, Y. Li, Z. Wang, and Y. Lu, 2022, 3-D numerical study on controlled source electromagnetic monitoring of hydraulic fracturing fluid with the effect of steel-cased wells: IEEE Transactions on Geoscience and Remote Sensing, **60**, 1–10, Art no. 4504210, doi: https://doi.org/10.1190/segam2021-3587537.1.

Li, W., D. Colombo, and E. Sandoval-Curiel, 2019, Deep learning-based EM inversion for reservoir monitoring: 89th Annual International Meeting, SEG, Expanded Abstracts, 5365–5369, doi: https://doi.org/10.1190/segam2019-w4-02.1.

Li, Y., and D. Yang, 2021, Electrical imaging of hydraulic fracturing fluid using steel-cased wells and a deep-learning method: Geophysics, **86**, no. 4, E315–E332, doi: https://doi.org/10.1190/geo2020-0178.1.

Liu, B., Q. Guo, S. Li, B. Liu, Y. Ren, Y. Pang, X. Guo, L. Liu, and P. Jiang, 2020, Deep learning inversion of electrical resistivity data: IEEE Transactions on Geoscience and Remote Sensing, **58**, 5715–5728, doi: https://doi.org/10.1109/TGRS.2020.2969040.

Puzyrev, V., 2019, Deep learning electromagnetic inversion with convolutional neural networks: Geophysical Journal International, **218**, 817–832, doi: https://doi.org/10.1093/gji/ggz204.

Wang, Z., G. Yu, L. Zhang, C. Wang, J. Zhang, and Z. Liu, 2017, The use of time-frequency domain electromagnetic technique to monitor hydraulic fracturing: SEG Technical Program, Expanded Abstracts, 1268–1273, doi: https://doi.org/10.1190/segam2017-17584035.1.

Wang, Z., G. Yu, L. Zhang, C. Wang, J. Zhang, and Z. Liu, 2019, The use of time-frequency domain EM technique to monitor hydraulic fracturing: Presented at the International Workshop on Gravity, Electrical & Magnetic Methods and Their Applications, 41–44, doi: https://doi.org/10.1190/GEM2019-011.1.


Downloaded 09/04/22 to 204.124.181.130. Redistribution subject to SEG license or copyright; see Terms of Use at http://library.seg.org/page/policies/terms
DOI:10.1190/image2022-3737841.1


© 2022 Society of Exploration Geophysicists and the American Association of Petroleum Geologists